The relationship between visible light emission and species fraction of the hydrogen ion beams extracted from 2.45 GHz microwave discharge

O. D. Cortázar, A. Megía-Macías, O. Tarvainen, T. Kalvas, and H. Koivisto

---

Articles you may be interested in

Ultra-fast intensified frame images from an electron cyclotron resonance hydrogen plasma at 2.45 GHz: Some space distributions of visible and monochromatic emissionsa)
Rev. Sci. Instrum. **85**, 02A902 (2014); 10.1063/1.4824812

Surfatron Plasma Source Working at Frequency 2.45 GHz for Technological Applications
AIP Conf. Proc. **812**, 72 (2006); 10.1063/1.2168800

A 2.45 GHz microwave negative hydrogen ion source
Rev. Sci. Instrum. **71**, 1042 (2000); 10.1063/1.1150381

Enhanced production of multi-charged ions using pulse-modulated microwave in a 2.45 GHz electron cyclotron resonance source
Rev. Sci. Instrum. **71**, 657 (2000); 10.1063/1.1150340

Role of low-energy electrons in Ar emission from low-pressure radio frequency discharge plasma
Appl. Phys. Lett. **75**, 328 (1999); 10.1063/1.124365

The relationship between visible light emission and species fraction of the hydrogen ion beams extracted from 2.45 GHz microwave discharge

O. D. Cortázar,[1,a)] A. Megía-Macías,[2,3] O. Tarvainen,[4] T. Kalvas,[4] and H. Koivisto[4]

[1]*Universidad de Castilla-La Mancha, INEI-Institute for Energy Research, Camilo José Cela s/n, 13170 Ciudad Real, Spain*

[2]*CERN, BE Department, CH1211 Geneva, Switzerland*

[3]*ESS Bilbao Consortium, Polígono Ugaldeguren-III Pol. A 7B, 48170 Zamudio, Vizcaya, Spain*

[4]*Department of Physics, University of Jyväskylä, P.O. Box 35 (YFL), 40500 Jyväskylä, Finland*

The relationship between Balmer-α and Fulcher-band emissions with extracted H^+, H_2^+, and H_3^+ ions is demonstrated for a 2.45 GHz microwave discharge. Ion mass spectra and optical measurements of Balmer-α and Fulcher-band emissions have been obtained with a Wien Filter having an optical viewport on the plasma chamber axis. The beam of approximately 1 mA is analyzed for different plasma conditions simultaneously with the measurement of light emissions both with temporal resolution. The use of visible light emissions as a valuable diagnostic tool for monitoring the species fraction of the extracted beams is proposed. © 2015 AIP Publishing LLC. [http://dx.doi.org/10.1063/1.4928475]

I. INTRODUCTION

Electron Cyclotron Resonance (ECR) plasma discharges are used widely in ion sources for accelerators as well as implantation industry.[1–3] For the hydrogen specific case, a profound interest on plasma processes determining the ion species fraction dynamics is emerging due to the necessity of H_2^+ and H_3^+ molecular ion beams for different applications from hadron therapy to neutrino experiments.[4–6] Recent results demonstrate the capabilities of the 2.45 GHz plasma sources for producing intense beams of molecular hydrogen ions.[7,8] On the other hand, visible light spectroscopy has been recently suggested as a non-invasive qualitative diagnostics for monitoring the plasma species fraction during ion source operation.[9] In order to collect experimental evidence, a Wien Filter ion velocity analyzer system with optical measurement capabilities has been developed. The results reported herein demonstrate the correlation between temporal evolution of H^+, H_2^+, and H_3^+ ion beam currents and filtered visible light emissions in a 2.45 GHz hydrogen plasma discharge.

II. EXPERIMENTAL SETUP

The plasma source dimensions and characteristics can be found in Ref. 10. The *plasma electrode, extraction system, and Wien Filter* subsystems were designed using the *IBSimu* code.[11] Fig. 1 shows the system cross section where solenoid pancakes and mechanical support frame have been removed for simplicity. The plasma electrode aperture is 1 mm in diameter and for this reason the system is pumped from both sides (rear and front) to reach a good background pressure in the plasma chamber. The plasma source is grounded while typical voltages of the puller (together with the filter body) is −10 kV.

The einzel electrode is polarized at +7.5 kV respect to the puller.

The Filter itself is composed by a vacuum chamber with two pumping ports and a frame supporting the permanent magnets and the electrostatic deflector plates. The scheme has the practical advantage that the frame can be easily mounted, pre-aligned, and checked outside of the vacuum chamber. Fig. 2 shows the frame structure in detail. The deflector plate alignment screws push the plates towards the axis while a spring in the center of the plate is used as recovery force. In the case of the magnets, the attractive magnetic force is used as recovery force while alignment screws are used to push them apart for precise positioning. The Wien Filter entrance aperture is 12 mm in diameter while the exit plate has a 4 mm collimating slit. The deflection plates are 110 mm long having 14 mm gap in between and can make a sweep from 0 to ±3000 *V* potential. The permanent magnets produce an uniform transverse magnetic field of 140 mT.

The Faraday's cup design is also shown in Fig. 1. Its body is made of copper and is electrically isolated from the Wien Filter body and the cup has an axial channel of 4 mm in diameter by 50 mm in length to allow optical observations. A repeller electrode is placed at the Faraday's cup input for reinserting the secondary electrons produced by ion impact avoiding the error on the currents reading. Moreover, a pair of magnets produce a transverse magnetic field to avoid particle losses by deflecting them before reaching the end of the channel.

The fact that the Wien Filter body is polarized at the extraction voltage while the plasma source is grounded implies that part of its electronic control-acquisition system must be floating at the same potential. Fig. 3 shows the scheme of the Wien Filter control-acquisition setup. The part that floats at the filter potential (−10 kV) is marked with a grey background. The rest is grounded and can be seen on the right part of the figure represented as a table with a computer and other instruments. The computer is connected to the

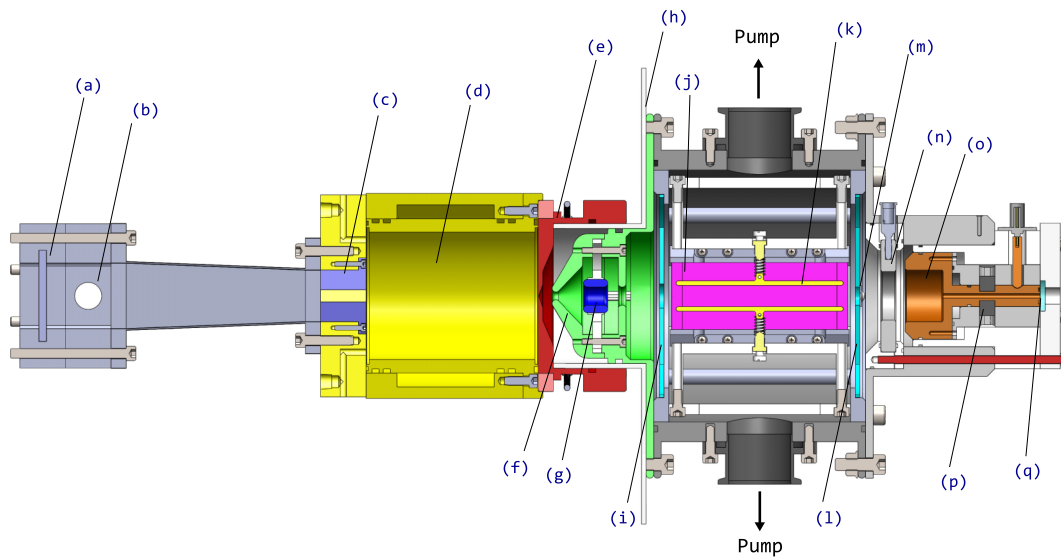a)Email address: daniel.cortazar@uclm.es

FIG. 1. A cross section view of the experimental setup where the solenoid coils and mechanical supporting frame have been removed for simplicity: (a) the quartz window, (b) rear pumping port, (c) microwave coupler, (d) plasma chamber, (e) plasma electrode, (f) puller electrode, (g) einzel electrode, (h) insulator piece, (i) Wien Filter entrance plate (magnetic steel), (j) NdFeB permanent magnets, (k) electrostatic deflection plates, (l) exit plate (magnetic steel), (m) exit slit, (n) secondary electron suppression electrode, (o) Faraday's cup, (p) deflection magnets, and (q) optical view port.

control unit by ethernet protocol via ethernet/optical converters (Eth/FO and FO/Eth) while the delay generator is connected via TTL-pulse/optical converters (TTL/FO and FO/TTL). Fiber optics links are used to communicate with the converters. Light emissions are collected through an optical collimator at the end of the Faraday's cup and conducted via fiber optics bundle to the photomultiplier tube (PMT). Optical filters can be placed in front of the PMT in order to record the light signal in specific wavelength ranges. The synchronization master pulses is based on the incoming power signal of a bidirectional coupler on the microwave injection wave-guide. The high voltage (HV) power supplies for the plates (-3 to $+3$ kV) and einzel electrode (7.5 kV) as well as the repeller power supply (80 V) are floating at the high voltage. The AC line power for feeding such subsystems is provided by a 1:1 transformer with HV isolation.

The instrument operation can be set in two acquisition modes: *spectrum* or *ion species evolution*. In the *spectrum* mode, the Wien Filter can obtain full spectra of (singly charged) ion mass in a range between 1 and 20 amu by sweeping the deflection voltage and simultaneously acquiring the current values from the Faraday's cup. This operation mode is designed to be used by obtaining data from different consecutive pulses. It implies that the reproducibility and stability must be kept in reasonable margins for obtaining representative data. The timing for the data acquisition must be specified to determine the instant at which the spectrum is obtained during each pulse.

Once the spectrum is obtained and the ion species are identified, the voltages corresponding to each species can be used in the *ion species evolution* mode. In this mode, the system can acquire *current vs. time* signals for fixed preselected voltages allowing to obtain the temporal response of each ion species to the discharge pulse with 1 μs resolution. Note that also in this mode, data are typically obtained and averaged from several consecutive pulses.
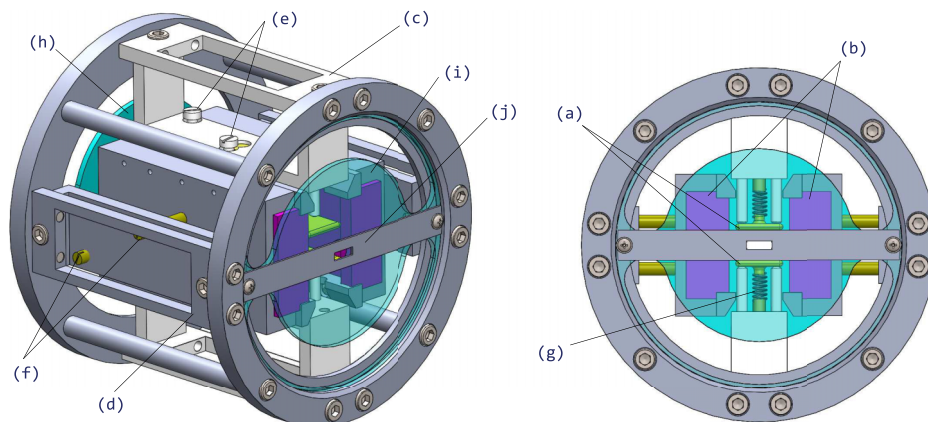

FIG. 2. Wien Filter: (a) electrostatic deflector plates, (b) permanent magnets, (c) deflector plate supporting bridge, (d) magnet supporting bridge, (e) deflector plate alignment screws, (f) magnet alignment screws, (g) plate positioning spring, (h) entrance plate, (i) exit plate, and (j) collimating slit.
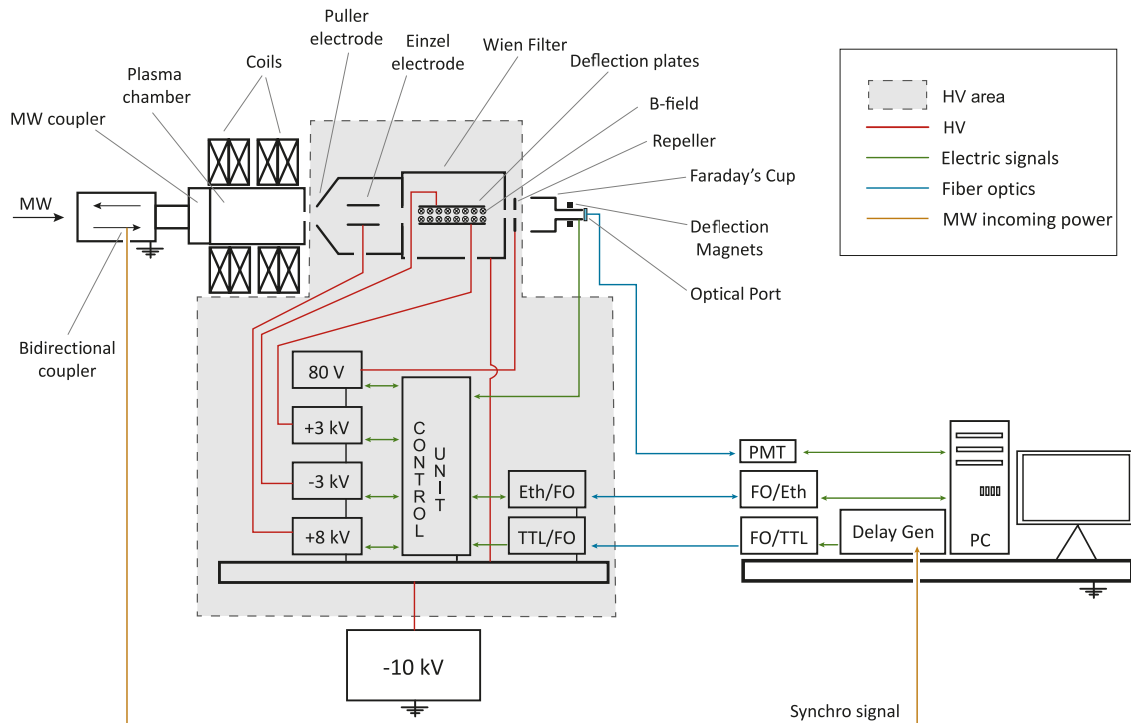
FIG. 3. Wien Filter control system diagram. Note that the plasma chamber is grounded while the Wien Filter analyser and its subsystems are polarized at -10 kV (shadow area).

III. SIMULATIONS AND RESULTS

Simulations of the Wien Filter output have been performed with *IBSimu code*[11] for different beam intensities and beam species fractions to verify that the observed ion fractions are representative of the extracted beam. Fig. 4 shows normalized simulated spectra for high (a) and low (b) ratios between H^+ ions and H_2^+ and H_3^+ ions superimposed to experimental spectra. The gas pressure, the absorbed power, and the magnetic field distribution in the plasma chamber have been observed to be the key factors for the ion ratios in the experimental spectra. The deflector voltages in the simulated and experimental spectra are within the 5% error margin that is set by the accuracy of the magnetic field simulation (Radia3D) and magnet grade tolerances. It is therefore concluded that the simulation reproduces the experimental spectrum. Note that in Fig. 4(a), some impurities in the range of 8-15 amu are recorded.

In order to confirm that the extracted species fraction is conserved during the transport through the filter, simulations were carried out with several total intensities (extracted from the source) and species fraction. Table I shows the extracted and transported species fractions through the Wien Filter for the more significant values of incoming P_i and reflected P_r power and coupling conditions. According to the simulation, the filter preserves the species fraction independent on the total intensity, i.e., the experimentally recorded spectra are believed to correspond to the species fractions extracted from the plasma source.

An important characteristic of the design is its capability of measuring light from the plasma simultaneously with the extracted ion species fraction. Fig. 5(a) shows a typical spectrum where H^+ and H_3^+ are clearly resolved. Fig. 5(b) shows
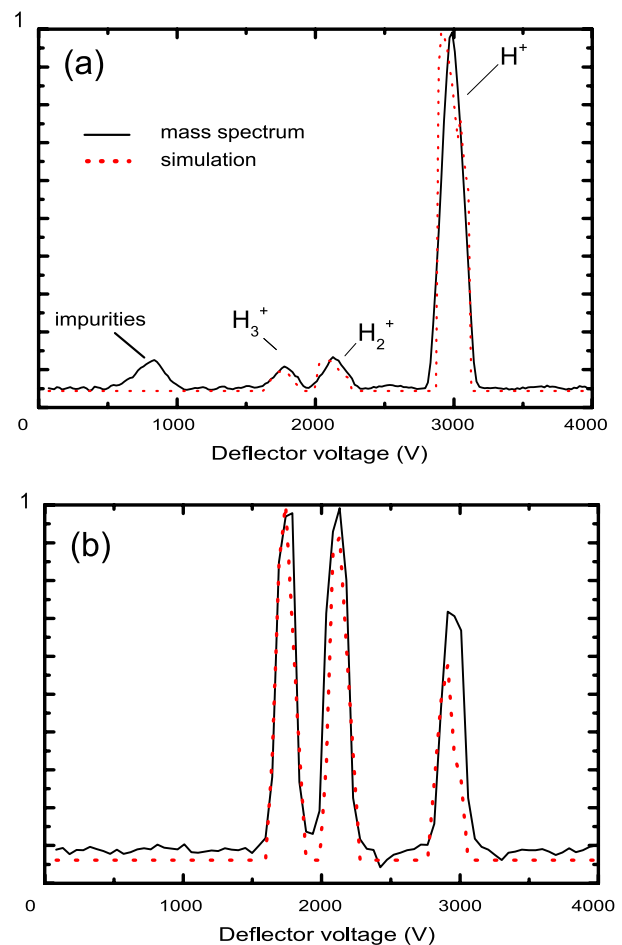

FIG. 4. Comparison between experimental and simulated spectra for high (a) and low (b) ratios of H^+ ions and H_2^+ and H_3^+ ions.

TABLE I. Simulation of extracted species fractions vs. the transported species fractions through the Wien filter for the more significant experimental conditions.

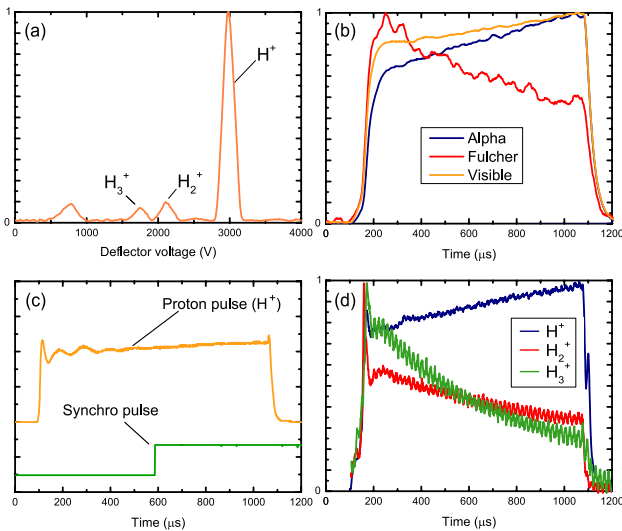| Power P_i (W)	Coupling $(P_i - P_r)/P_i$ (%)	Beam intensities (mA)	Extracted fractions (%) $H^+/H_2^+/H_3^+$	Transported fractions (%) $H^+/H_2^+/H_3^+$
600	70	0.63	89/7/4	89.5/6.7/3.8
900	40	0.31	89/7/4	89.5/6.7/3.8
1500	10	0.16	89/7/4	89.5/6.7/3.8
1500	10	0.63	80/10/10	80.9/9.6/9.6
1300	40	0.63	20/40/40	21.2/39.8/39

FIG. 5. Typical spectrum (a), timing signal respect to proton pulse (b), visible signals (c), and species current pulses (d).
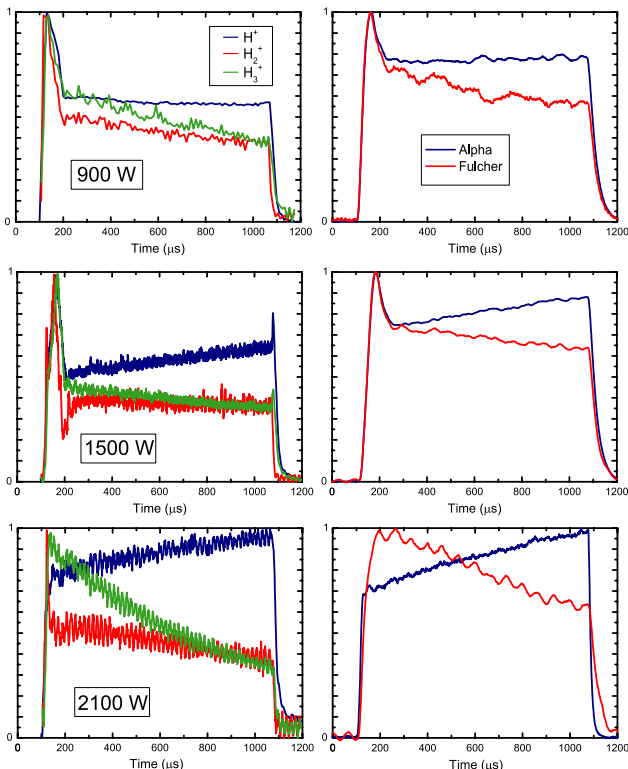

FIG. 6. A comparison of H^+, H_2^+, and H_3^+ currents and Balmer-α and Fulcher signals for 900, 1500, and 2100 W of incoming power. All signals are normalized.

the temporal evolution of Balmer-α (filter 660 nm FWHM 10 nm), Fulcher (filter 600 nm FWHM 40 nm) band, and integrated visible light where the filters were selected by availability and well positioned wavelength expecting a good transmission response as was demonstrated in previous works.[9] Fig. 5(c) shows the corresponding timing signal where the rise of the synchro pulse indicates the instant of data recording with respect to the proton pulse and Fig. 5(d) the temporal evolution of the ion species currents of H^+, H_2^+, and H_3^+. Fig. 6 shows a comparison between normalized ion currents and optical signals for three incoming microwave powers of 900, 1500, and 2100 W to test the resolving power under different conditions. It should be noted that the temporal behaviour of Balmer-α signal is similar to H^+ current signal and Fulcher band emission to H_2^+ and H_3^+ ion currents, specially H_2^+.

IV. DISCUSSION AND CONCLUSIONS

Balmer-α and Fulcher band emissions have been previously studied with the same 2.45 GHz plasma source in connection with plasma distributions.[9,12,13] The present system allows to measure the ion species current evolutions of H^+, H_2^+, and H_3^+ and directly to compare them with simultaneous optical measurements. The measurements shown in Figs. 5 and 6 give qualitative experimental evidence of the similar temporal evolution of the ion species currents and Balmer-α and Fulcher band emissions. Note the peaks of current during the breakdown with a duration of 100 μs for the cases of 900 and 1500 W. These peaks that have been reported previously associated to a temperature peak[8,16] are also well reflected in the light signals.

According to the results, Balmer-α emission could be used as a representative signal of proton population in the plasma and the Fulcher band signal as a representative indication of molecular H_2^+ and H_3^+ ion production.

An explanation can be found in the basic processes resulting to visible light emission from the hydrogen plasma, i.e., the excitation of neutral hydrogen atoms and molecules by electron impact from level q to level p and the decay into level k by spontaneous emission resulting in line emission pk. The hydrogen Balmer series corresponds to the transitions from the excited states of atomic hydrogen with the primary quantum number $n_p > 2$ to the excited state with $n_k = 2$. Balmer-alpha radiation at 656.3 nm is emitted when $n_p = 3$ as the main transition within the Balmer-series. Hence, during the plasma ionizing phase, the Balmer-alpha emission is directly proportional to the density of atomic hydrogen which is also

true for electron impact ionization.[14] It is noteworthy that the cross section of $e + H_2 \rightarrow H_2^+$ is an order of magnitude larger than the cross section of $e + H_2 \rightarrow H^+$. This together with the fact that the extracted current of H^+ often exceeds the extracted current of H_2^+ implies that the dissociation degree of the neutral gas is very high. It has been argued that the main dissociation channel of the molecules in hydrogen discharges is electronic excitation to triplet states eventually decaying to repulsive $b^3\Sigma_u^+$-state.[15] The cross section for the triplet excitation peaks below 20 eV electron energy[14] and exceeds the molecular ionization cross section at energies <25 eV. Typical electron temperature in the 2.45 GHz microwave discharge has been measured to be 5–18 eV,[16] i.e., it can be argued that most electron impact processes lead to dissociation of the hydrogen molecule and further ionization to H^+, which would explain the significant fraction of atomic ions in $e + H \rightarrow H^+ + 2e$.

The Fulcher-band emission around 600 nm corresponds to the molecular triplet transition $d^3\Pi_u \rightarrow a^3\Sigma_g^+$ with a further transition (emission in UV) $a^3\Sigma_g^+ \rightarrow b^3\Sigma_u^+$ to a repulsive state.[17] Thus, Fulcher-band emission indicates dissociation of the emitting molecule.

The main channels of molecular ion production are[14] $e + H_2 \rightarrow H_2^+$ and $H_2^+(\nu) + H_2 \rightarrow H_3^+ + H$. Thus, a plausible explanation for the gradual decrease of the molecular ion signals and Fulcher's band emission could be the gradual decrease of the (molecular) gas density in the discharge chamber. Such effect can take place due to heating of the neutral gas or neutral starvation. The fact that the H_3^+ ion current exhibits a stronger temporal dependence (gradual decrease in Fig. 6) supports this interpretation. This is because the production rate of H_3^+ is proportional to both the neutral molecule H_2 and molecular ion H_2^+.

The relationship between the optical emissions and ions species demonstrated in this paper has interesting applications as a quick, inexpensive, and non-invasive diagnostics for hydrogen plasma ion sources. In particular, it allows monitoring the temporal stability and pulse-to-pulse reproducibility of a hydrogen ion source (in terms of species fraction) without interrupting the extracted ion beam. Such capability could be beneficial for an ion source serving as an injector for an accelerator or an application requiring high temporal stability. For such applications, the system could be improved by utilizing a splitted fiber optics bundle coupled to optical filters. Such

setup can acquire both the atomic and molecular light signals for monitoring purposes.

On the other hand, these results complement previous studies on the plasma light spatial distributions that show how the molecular dissociation and atom excitation dynamics take place in the time and in the space during plasma transients.[9,13] In addition, the use of this diagnostics as a simple and direct research tool could permit a rapid and inexpensive way to study and optimize new designs of hydrogen plasma sources for special applications, i.e., where molecular ion production is pursued.

[1]R. Gobin, N. Chauvin, O. Delferrière, T. O., and D. Uriot, in *Proceedings of LINAC2012* (Tel-Aviv, Israel, 2012).
[2]M. Cao, J. Cheng, C. Han, and L. Ji, Adv. Mater. Res. **1006**, 193 (2014).
[3]J. Pelletier and A. Anders, IEEE Trans. Plasma Sci. **33**, 1944 (2005).
[4]R. Gobin, V. Blideanu, D. Bogard, G. Bourdelle, N. Chauvin, O. Delferrière, P. Girardot, J. Jannin, S. Langlois, D. Loiseau, B. Pottin, J.-Y. Rousse, and F. Senée, Rev. Sci. Instrum. **81**, 02B301 (2009).
[5]J. Alonso, W. Barlleta, M. Toups, J. Conrad, Y. Liu, M. Bannister, C. Havener, and R. Vane, Rev. Sci. Instrum. **85**, 02A509 (2014).
[6]J. Alonso, L. Calabreta, D. Campo, L. Celona, J. Conrad, R. Martinez, R. Jhonson, F. Labrecque, M. Toups, D. Winklehner, and L. Windslow, Rev. Sci. Instrum. **85**, 02A752 (2014).
[7]Y. Xu, S. Peng, H. Ren, J. Zhao, J. Chen, T. Zhang, A. Zhang, Z. Guo, and J. Chen, Rev. Sci. Instrum. **79**, 02B713 (2008).
[8]R. Xu, S. Peng, Z. Yuan, Z. Song, J. Yu, and Z. Guo, Rev. Sci. Instrum. **85**, 02A943 (2014).
[9]O. D. Cortázar, A. Megía-Macías, O. Tarvainen, A. Vizcaíno-de-Julián, and H. Koivisto, Plasma Sources Sci. Technol. **23**, 065028 (2014).
[10]A. Megía-Macías, O. D. Cortázar, and A. Vizcaíno-de Julián, Rev. Sci. Instrum. **85**, 033310 (2014).
[11]T. Kalvas, O. Tarvainen, T. Ropponen, O. Steczkiewicz, J. Arje, and H. Clark, Rev. Sci. Instrum. **81**, 01B703 (2010).
[12]O. Cortázar, A. Megía-Macías, A. Vizcaíno-de Julián, O. Tarvainen, J. Komppula, and H. Koivisto, Rev. Sci. Instrum. **85**, 02A902 (2014).
[13]O. Cortázar, A. Megía-Macías, O. Tavainen, and H. Koivisto, Nucl. Instrum. Methods Phys. Res., Sect. A **781**, 50 (2015).
[14]R. Janev, D. Reiter, U. Samm, and O. Marchuk, J. Plasma Fusion Res. Ser. **7**, 319 (2006).
[15]R. Celiberto, R. Janev, A. Laricchiuta, M. Capitelli, J. Wadehra, and D. Atems, At. Data Nucl. Data Tables **77**, 161 (2001).
[16]O. Cortázar, A. Megía-Macías, and A. Vizcaíno-de Julián, Rev. Sci. Instrum. **83**, 3302 (2012).
[17]U. Fantz and D. Wűnderlich, At. Data Nucl. Data Tables **92**, 853 (2006).